Proc. Natl. Acad. Sci. USA
Vol. 86, pp. 7866–7870, October 1989
Biophysics

ATP-sensitive K^+ channels in a plasma membrane H^+-ATPase mutant of the yeast *Saccharomyces cerevisiae*

(patch clamp/proton pump/potassium transport/plasma membrane ATPase)

J. A. RAMIREZ†, V. VACATA†, J. H. MCCUSKER‡§, J. E. HABER‡, R. K. MORTIMER†, W. G. OWEN†, AND H. LECAR†

†Department of Biophysics and Lawrence Berkeley Laboratory, University of California, Berkeley, CA 94720; and ‡Rosenstiel Center, Department of Biology, Brandeis University, Waltham, MA 02254

Communicated by William A. Hagins, March 31, 1989 (received for review February 1, 1988)

ABSTRACT **A mutant in the plasma membrane H^+-ATPase gene of the yeast *Saccharomyces cerevisiae* with a reduced H^+-ATPase activity, when examined at the single-channel level with the patch-clamp technique, was found to exhibit K^+ channels activated by intracellular application of ATP. In the parent strain, the same channel, identified by its conductance and selectivity, is not activated by ATP. This activity in the mutant is blocked by the ATPase inhibitor *N,N'*-dicyclohexylcarbodiimide. ADP and the ATP analog adenosine 5′-[γ-[^{35}S]thio]triphosphate do not activate the channel. These findings suggest a tight physical coupling between the plasma membrane ATPase and the K^+ channel.**

The plasma membrane ATPase of yeast is a 100-kDa essential protein that functions as an electrogenic proton pump (1, 2), playing a major role in the regulation of intracellular pH and membrane potential. DNA sequence analysis (3) of the *PMA1* gene that encodes this H^+-ATPase has shown its homology to various H^+/K^+, Na^+/K^+, and Ca^{2+}-ATPases. Several lines of evidence (1, 2) suggest that the proton pump is indirectly coupled to a K^+-transport system. The transport system responsible for potassium uptake in yeast is known to have multiple affinities (4), and we seek to determine the role played in this process by the recently observed voltage-gated potassium channels (5). We report here patch-clamp experiments (6) on mutant yeast that reveal an unexpected interaction between a voltage-gated K^+ channel and the proton-pumping ATPase.

Recently McCusker *et al.* (7) isolated a large number of mutations in *PMA1*, the plasma membrane ATPase gene in the yeast *Saccharomyces cerevisiae*. The mutations were isolated by their resistance to hygromycin B. The ATPase activity of the *pma1* mutants is reduced by as much as 75%. These mutants are highly pleiotropic, exhibiting pH, osmotic, and cold sensitivity. Three severely affected mutants, including the *pma1-105* mutant discussed here, were unable to grow at pH 3.5 or with NH_4^+. These severe phenotypes are suppressed by adding 50 mM KCl, but not by NaCl, to the medium. Further analysis has shown that *pma1* mutant cells have reduced membrane potentials (8). The *PMA1*-encoded protein probably functions as a dimer or higher-order structure because the 53 *pma1* mutants display a complex pattern of intragenic complementation. Some combinations of *pma1* alleles complement for hygromycin B resistance (7), whereas others exhibit negative complementation, such that a diploid heterozygous for two mutant proteins is unable to grow (H. Cooper and J.E.H., unpublished work).

RESULTS

The *pma1-105* mutation exhibits a 65% reduction in ATPase activity (7). Biochemical analysis shows that the mutant protein is present in the plasma membrane at wild-type levels but exhibits an altered pH optimum, insensitivity to vanadate inhibition, and altered K_m for ATP (D. S. Perlin, J.H.McC. and J.E.H., unpublished work). The mutant results from a base substitution of Ser-368 to phenylalanine (S. Harris and J.E.H., unpublished results).

K^+ channels in the *pma1-105* mutant exhibit a surprising activation induced by micromolar concentrations of intracellular ATP. The K^+ channel of the *Pma*$^+$ parent strain, as well as that of other wild-type strains, does not exhibit the same sensitivity. Perfusion of two inside–out patches of *pma1-105* with ADP (1 mM) and two patches with the ATP analog adenosine 5′-[γ-[^{35}S]thio]triphosphate (1 mM) for 5 min did not activate the channel. In these experiments the same patches were perfused with 200 μM ATP before and after the analogs, clearly activating the channels.

Fig. 1 shows a typical record of patch-clamp currents for the mutant *pma1-105* before and after adding ATP. Perfusion of the patch with micromolar concentrations of ATP increases channel activity at both positive and negative voltages. This effect is reversible, as shown in Figs. 1 *C* and *E*, where ATP is removed from the perfusate. The ATP-activated channels of the mutant are blocked by *N,N'*-dicyclohexylcarbodiimide (DCCD) (20 μM), a proton-pump inhibitor, in <10 sec (Fig. 2). Inside–out patches of the *Pma*$^+$ parent strain perfused for 5 min with increasing ATP concentrations (10 μM, 20 μM, 50 μM, 100 μM, and 5 mM) fail to exhibit activation (Fig. 4) and are not blocked by DCCD.

Single-channel records and current–voltage curves in the absence of ATP are shown for mutant and parent strain in Fig. 3, showing unit conductance of 17 pS. Rapid flickering of a large number of open channels in a patch, produced by ATP concentrations of 50 μM or more, makes it difficult to resolve individual events. To further compare the channels in the wild-type and mutant strains, we constructed a library of isolated events for voltages between −120 and +120 mV. The isolated events show four distinct values of conductance: 17, 34, 49, and 67 pS. These values are multiples of the single-channel conductance of the K^+ channel identified in both the mutant and the parent strain *Pma*$^+$. The channel observed in the *pma1-105* mutant, therefore, has approximately the same conductance as the voltage-gated K^+ channel reported by Gustin *et al.* (5) for the wild type. The channel reported here, however, is activated by both depolarizing and hyperpolar-

The publication costs of this article were defrayed in part by page charge payment. This article must therefore be hereby marked "*advertisement*" in accordance with 18 U.S.C. §1734 solely to indicate this fact.

Abbreviation: DCCD, *N,N'*-dicyclohexylcarbodiimide.

§Present address: Department of Biochemistry, Stanford University School of Medicine, Palo Alto, CA 94305.

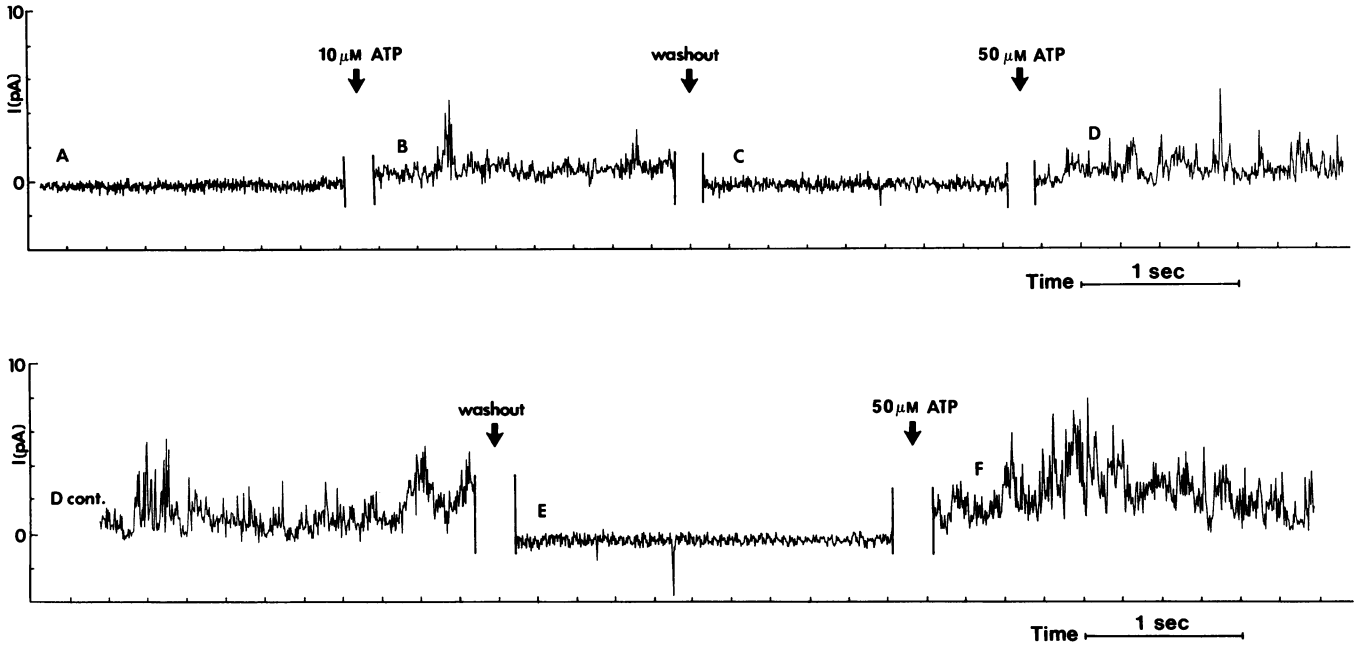

FIG. 1. Activation of K^+ channels by ATP in the *pma1-105* strain Y55-307. Pipette solution (solution 1, outside) is 150 mM KCl/5 mM NaCl/1.5 mM $MgCl_2$/1.5 mM $CaCl_2$/100 mM sorbitol/5 mM Hepes/50 μM ATP or 10 μM ATP (as indicated), pH 7.2. Traces: A, baseline noise; B, channels are activated by perfusion with 10 μM ATP/solution 1; C, activity decreased after ATP washout; D, activity recovered after perfusing with 50 μM ATP/solution 1; E, baseline noise recovered after ATP washout; F, activity regained with 50 μM ATP. Pipette voltage, 59 mV.

izing voltages in excess of 100 mV. The two-sided gating is, however, similar to that of the gated K^+ channel recently seen in plant guard cells (9).

The probability of a channel being open as a function of voltage was measured for both the mutant and the parent strain by two separate procedures that gave identical results. When individual channel events could not be resolved because of excessive activity of several flickering channels, we used the mean current in response to voltage steps and the steady-state noise to establish the probability of a channel being open as a function of voltage. This analysis, which is detailed in the *Appendix*, shows that the voltage-dependent probability of being in the open state saturates at high voltage to a maximum value of <0.1, as is suggested by the single-channel records of Fig. 3. This approach, in turn, requires the channel activation kinetics to have both a voltage-dependent and a voltage-independent component.

Fig. 4 shows voltage-clamp records for the wild-type channels without ATP and with 1 mM ATP in the bathing medium. Onset of channel activity coincides with increase in membrane noise. The probability of being in the open state is obtained from these data by measuring the normalized voltage-dependent conductance and also by analyzing the current–noise variance. Computer averaging over hundreds of these records for five different experiments yields the voltage-dependent open-state probability in Fig. 4*C*, which shows no discernible difference without or with ATP (0.1 mM). Similar results were obtained on three separate patches.

Fig. 5 shows the response of a typical membrane patch of the *pma1-105* mutant to various concentrations of ATP (0, 100, 500, and 1000 μM). Fig. 5 *A–D* shows that the voltage region of intense channel-gating activity is shifted to lower values of voltage as ATP concentration is increased in the medium. The open-state probability is plotted in Fig. 5*E* for the two extreme ATP concentrations—0 and 1 mM. As a consequence of ATP addition, the probability curve is shifted to lower values of membrane potential by ≈50 mV. A similar shift was obtained in five separate patches.

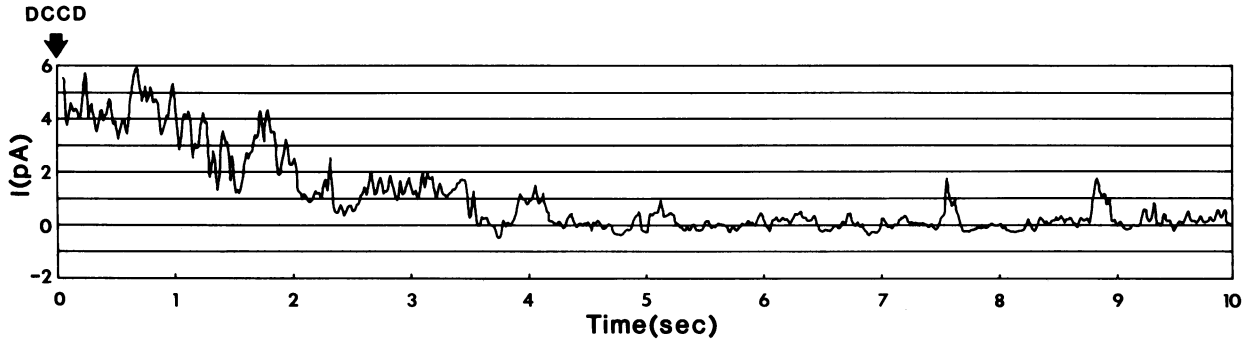

FIG. 2. Stepwise relaxation of patch current after DCCD application. The horizontal lines represent the single-channel conductance at the given potential. Ionic solutions and voltage are the same as in Fig. 1. The signal has been averaged over intervals of 10 msec. In this case, four channels are blocked by 20 μM DCCD in 10 mM ATP. At 120 mV DCCD blocks an average of 10 channels in a patch. Currents of 10–20 pA are typically induced in the patches by increasing pipette voltage to 100 mV in either the positive or negative direction. The patch current has rectification properties that parallel the gating of the individual channels. Therefore, this current results from the action of an average of 5–10 channels in the patch. The stepwise relaxation of the average current after the addition of DCCD proceeds in jumps equal to the unit single-channel current.

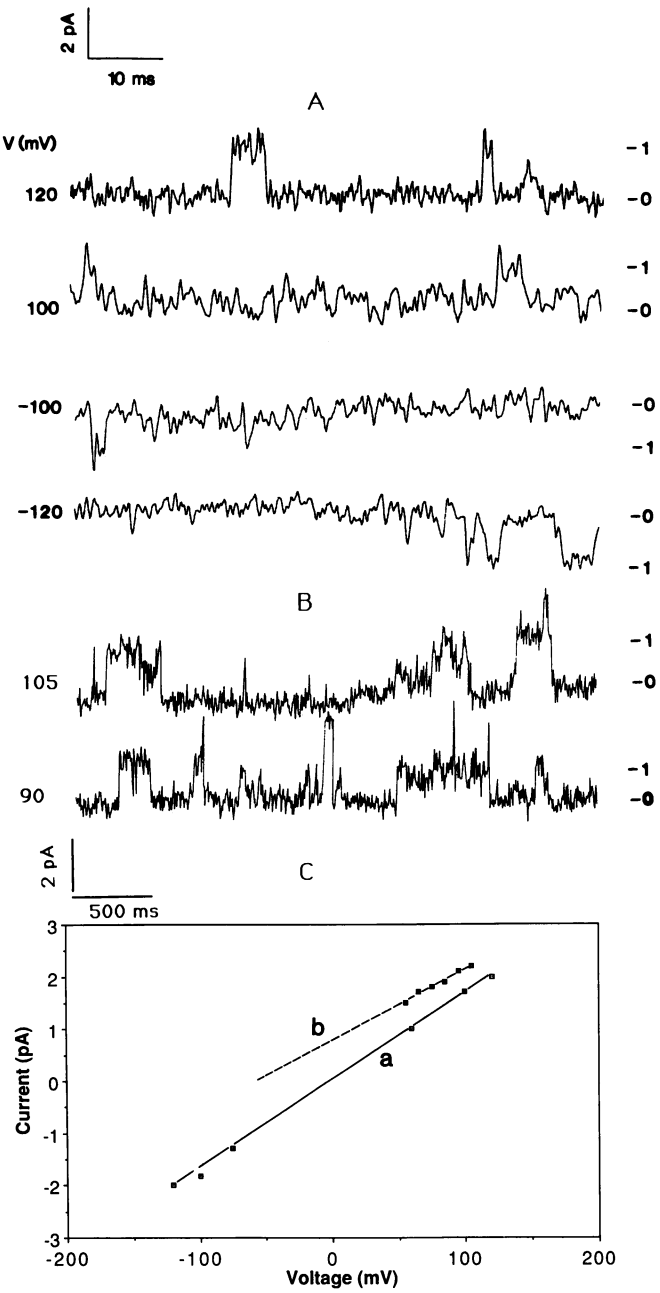

FIG. 3. (*A*) Single-channel events for the *pma1-105* mutant. Pipette solution = external solution = solution 1 as in Fig. 1 with no ATP. (*B*) Single-channel events for the parent strain *Pma*$^+$. Pipette solution is solution 1. External solution is 5 mM KCl/140 mM NaCl/1.5 mM $MgCl_2$/1.5 mM $CaCl_2$/100 mM sorbitol/5 mM Hepes, pH 7.2. (*C*) *I–V* curves generated by the *pma1-105* mutant and the parent strain *Pma*$^+$, which show a conductance of 17 pS (*pma1-105*) with solution 1 inside and outside the pipette (*a*), and 13 pS (*Pma*$^+$) (*b*) and an interpolated reversal potential of −58 mV with solution 1 inside and solution 2 (10 mM KCl/140 mM NaCl/1.5 mM $CaCl_2$/1.5 mM $MgCl_2$/100 mM sorbitol/5 mM Hepes, pH 7.2) outside the pipette.

DISCUSSION

These experiments show how a mutation in the gene that codes for the plasma membrane ATPase affects the gating of a voltage-gated K^+ channel. The *pma1-105* mutation exhibits two effects related to ATP—decreased plasma-membrane ATPase activity, and ATP-dependent gating of the K^+ channel. In the absence of ATP, the gating and unit conductance of the channel are the same as in *Pma*$^+$.

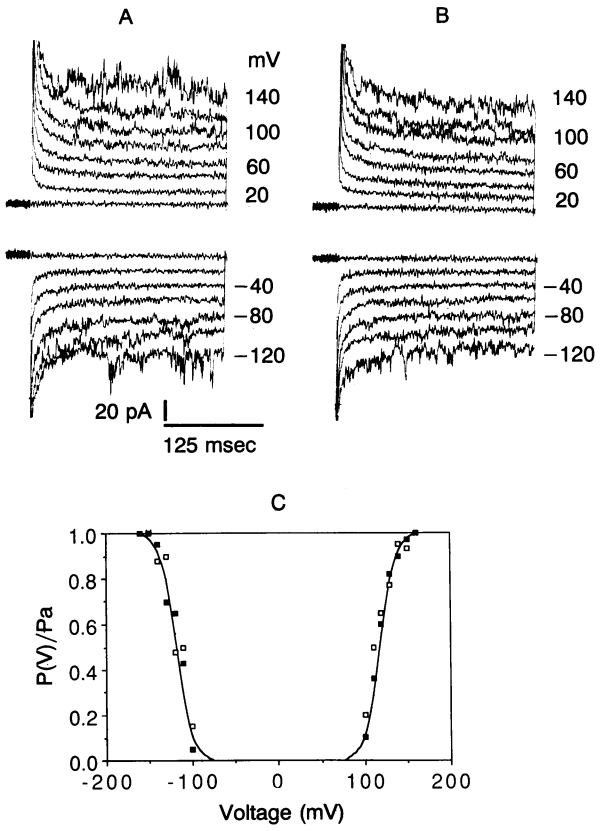

FIG. 4. Effect of ATP on the parent strain *Pma*$^+$. Solution 1 both inside and outside the pipette. (*A*) Typical sequence of positive (pipette) and negative voltage steps from −120 to 140 mV in the inside–out configuration produces the currents shown here. No ATP in the bathing media. The normal gating of the channel is evident for voltages, $V < -100$ mV or $V > 100$ mV. (*B*) Same as in *A*, except that the external bath contains 1 mM ATP. No significant difference is detected when compared with *A*. (*C*) By using a procedure detailed in the *Appendix*, the ratio of the probability of being open to its asymptotic value (*R*) is calculated. □, *R* for both hyperpolarizing and depolarizing voltages when ATP concentration is zero; ■, *R* for ATP concentration of 100 μM. The lines are the analytical fits to the function $p(V) = p_a(1/\{1 + (1 - p_a)\exp-[\beta(V - V_0)]\})$, with $p_a = 0.1$, $\beta = 0.115\ (\text{mV})^{-1}$, and $V_0 = 120$ mV (see *Appendix*). Each data point was obtained by computer averaging of ten traces of 1-sec duration for each voltage; digitization rate was 3 kHz.

The *pma1* mutation is known to affect ATPase activity and occurs at a 10-amino acid separation from the phosphorylation site. How this mutation might exert an indirect effect on the voltage-sensitive K^+ channel can be envisioned. For example, the altered ATP binding at the densely packed ATPase sites might lead to altered membrane surface-charge density in the vicinity of the channels. Surface-charge shift would be consistent with the altered K_m of the highly charged ATP but is not consistent with our findings that high concentrations of ATP analogs do not activate the channel and that ATP has no effect on the gating of the channel in the parent strain.

In addition, ATP shifts the probability-of-opening curve to lower absolute values of potential at both positive and negative voltages. This result would not be expected for a surface-charge effect, regardless of whether the two gating regions stem from two separate channels or from different open states of the same channel because the ATP binding is only at one surface of the membrane. Shifting of the open-state probability with voltage, as a function of ATP concentration, follows Michaelis–Menten kinetics with half saturation around 500 μM, which is very close to the altered K_m for the mutant *pma1-105*.

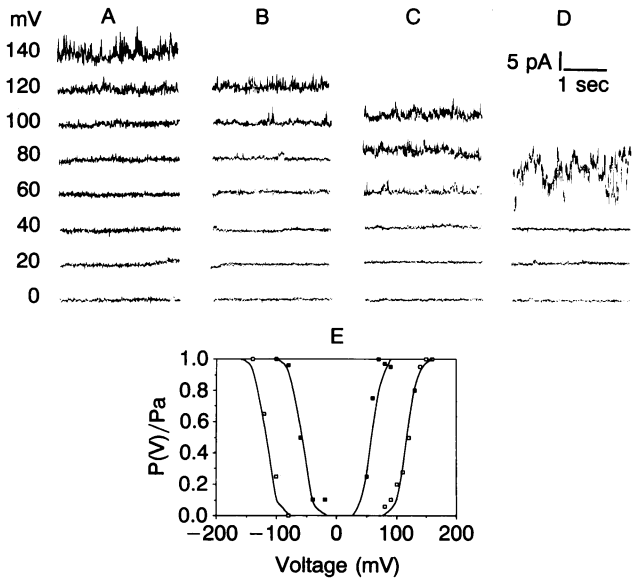

FIG. 5. Effect of increasing ATP concentration in the mutant *pma1-105* K^+ channel. Pipette solution = 100 mM KCl/5 mM NaCl/1.5 $CaCl_2$/1.5 $MgCl_2$/100 mM sorbitol/5 mM Hepes, pH = 7.3. Outside solution = 25 mM KCl/80 mM NaCl/1.5 $CaCl_2$/1.5 $MgCl_2$/100 sorbitol/10 mM Hepes, pH = 7.3. (*A*) No ATP in bath solution. The different traces show the normal gating of the mutant with increased positive voltage. This positive voltage corresponds to a negative voltage with respect to ground when the cell membrane is intact (hyperpolarizing voltage). (*B*) Outside of the cell is now perfused with the same solution plus 100 μM ATP; the channel starts gating at lower voltages. (*C*) Same as for *B* but with 500 μM ATP; the voltage where the channel starts gating decreases further. (*D*) ATP concentration increased to 1 mM; gating occurs at ≈50 mV. (*E*) By using a procedure detailed in the *Appendix*, ratio of the probability of being open to its asymptotic value (R) is calculated. □, R for both hyperpolarizing and depolarizing voltages when ATP concentration is zero. V_0 = 120 mV; ■, R for an ATP concentration of 1 mM. V_0 = 60 mV. The lines are the analytical fits of the points to the function $p(V) = p_a(1/\{1 + (1 - p_a)\exp-[\beta(V - V_0)]\})$, with $p_a = 0.1$ and $\beta = 0.115\ (mV)^{-1}$. Data points were again obtained by computer averaging of ten traces of 1-sec duration for each voltage; digitization rate was 3 kHz.

Alternatively, ATP-dependent perturbations could occur if a K^+ channel, tightly surrounded by a cluster of H^+-ATPase molecules, were exposed to altered solution pH induced by changes in ATPase activity. Solution pH changes are unlikely for an excised inside–out patch of membrane, unless it has been sucked deeply into the pipette.

Because the mutation in *pma1-105* is specifically in the *PMA1* gene, which codes for the ATPase, the effect on the channels is not likely to come from ATP reception by an autonomous channel, unless this, too, is coded by the same gene. Although ATP has been shown to close K^+ channels of animal cells (10, 11), ATP has not been shown to enhance channel opening.

The possibility remains that the K^+ channel might actually be some transiently induced pathway related to the multimeric ATPase itself. Although evidence exists for a H^+/K^+ electroneutral exchange mechanism (1, 10–12), such coupling has been seen mainly at the membrane resting potential, for which the wild-type K^+ channel is open only a short time.

Our observations might be combined with evidence that purified ATPase from a different yeast, *Schizosaccharomyces pombe*, transports K^+ coupled to ATP hydrolysis (13) to support the idea that the K^+ channel resides in a protein coded by the *PMA1* gene. However, even if this were so, there is no evidence that potassium channels equal ATPase sites in number; there appear to be far fewer potassium channels than pumps. Thus, either the channels affected by the mutation are different membrane proteins that are merely in proximity to the ATPases, or the observed potassium channel events are caused by some "leaky" variant conformation adopted by a small fraction of the ATPases.

If the plasma membrane ATPase in yeast, functioning as an electrogenic pump, should also be the site of an inefficient H^+/K^+ transporter or a voltage-regulated K^+ channel, then possibly the protein of the *pma1-105* mutant fails to change conformation as rapidly as the wild-type protein, allowing a greater flux of K^+ into the cell. The increased K^+ influx may explain our observation that the predominant effect of *pma1-105* and other *pma1* mutants is not to significantly reduce proton efflux from the cell but to markedly reduce the cell membrane potential (8). The strong homology between the yeast *PMA1* gene and the H^+/K^+ and Na^+/K^+-ATPases of higher organisms suggests that they work similarly, but in yeast the K^+ transporter function has been largely, but not completely, decoupled from the proton pump. Indeed, one of the mutants we have studied, *pma1-114*, has normal ATPase activity but very low membrane potential (8).

APPENDIX

Noise Analysis of Channel-Gating Kinetics. Figs. 4 and 5 show voltage-clamp currents for membrane patches containing several channels. Channel gating is manifest in both the steep region of voltage-dependent conductance and the current–noise fluctuations. At each voltage the mean current and current–noise variance were measured and fit to a self-consistent scheme of voltage-dependent gating.

Under the assumption that the channels have a minimal gating scheme of three states (two closed and one open) with one transition being voltage dependent and the other not, gating obeys the following rate equation:

$$\text{closed (2)} \underset{w_{12}(V)}{\overset{w_{21}(V)}{\rightleftharpoons}} \text{closed (1)} \underset{w_{01}}{\overset{w_{10}}{\rightleftharpoons}} \text{open (0)}, \qquad [1]$$

where w_{ij} are the transition rates as shown. The steady-state probability of being in the open state is given by

$$p(V) = \{1 + (w_{01}/w_{10})[1 + w_{12}(V)/w_{21}(V)]\}^{-1}. \qquad [2]$$

Assuming the states separated by voltage-dependent transitions are in a Boltzmann distribution in equilibrium, the voltage-dependent rates are related by

$$w_{12}(V)/w_{21}(V) = \exp[-(Q/kT)(V - V_0)], \qquad [3]$$

where Q is the effective gating charge and V_0 is the potential for which p is half maximum. Thus $p(V)$ can be written as

$$p(V) = p_a\{1 + (1 - p_a)\exp[-(Q/kT)(V - V_0)]\}^{-1}, \qquad [4]$$

where $p_a = w_{10}/(w_{10} + w_{01})$ is the maximum probability of being open.

For N independent, identical channels, the mean, $\langle I\rangle$, and the variance, $\mathrm{Var}_I(V)$, of the current fluctuations are given by

$$\langle I\rangle = N\gamma(V - E)p, \qquad [5a]$$

$$\mathrm{Var}_I(V) = \langle I^2 - \langle I\rangle^2\rangle = N[\gamma(V - E)]^2p(1 - p), \qquad [5b]$$

where γ is the single-channel conductance, E is the reversal potential, and p is the probability function given by Eq. **4**.

The observed current variance can be used to obtain an independent value for p_a, the maximum probability of being open. To do this, we use the observable quantity $\mathrm{Var}_I(V)/(V - E)^2$ as a measure of the quantity $F(V) = p(1 - p)$. At large

depolarizations $F(V)$ has an asymptotic value $F_a = p_a(1 - p_a)$, so that from Eq. **5b** we get

$$\frac{F(V)}{F_a(V)} = \frac{p(1-p)}{p_a(1-p_a)} = \frac{\mathrm{Var_I}(V)/(V-E)^2}{\mathrm{Var_I}(V^*)/(V^*-E)^2}, \quad [6]$$

where V^* is the voltage at which the asymptotic value is determined ($V^* = 140$ mV).

The observed and calculated values of $F(V)/F_a(V)$ are plotted in Fig. 6 as a function of membrane potential. A family of curves is shown for varying values of p_a. The experimental data points are fit well by a value of $p_a \leq 0.1$. The inset in Fig. 6 shows the fit of the function $p(V)/p_a(V)$, with $p_a = 0.1$. The

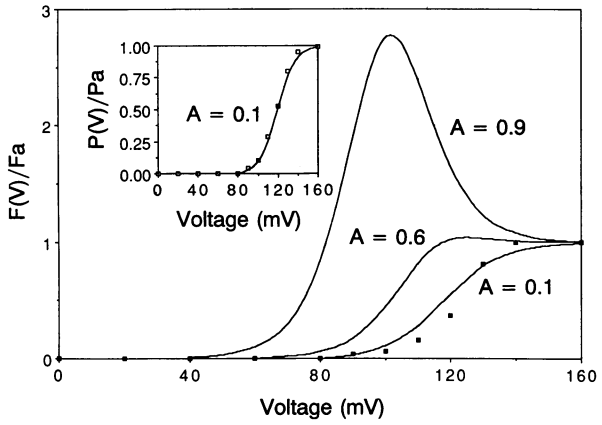

FIG. 6. Analysis of single-channel conductance using voltage-dependent current noise. The voltage dependence of the current noise is fit to the kinetic scheme of Eq. **1**. This implies a functional form for the variance, $F(V) = p_a(1 - p_a)\{1 + \exp[-\beta(V - V_0)]\}(1/\{1 + (1 - p_a)\exp[-\beta(V - V_0)]\})$. The parameter A represents the test values for p_a. The ratio of $F(V)/F_a$ is shown as a function of voltage. □, Data obtained from mutant *pma1-105*. Three different curves for values of $p_a = 0.9$, 0.6, and 0.1 show that only small values of p_a fit the data. A good fit is obtained for $p_a \leq 0.1$, $\beta = 0.115$ (mV)$^{-1}$, $V_0 = 120$ mV. (*Inset*) Fit for the probability of being open, $p(V) = p_a(1/\{1 + (1 - p_a)\exp[-\beta(V - V_0)]\})$, using the same parameter values as those used to fit $F(V)$.

joint fit shows that the noise variance and the steady-state probability of being in the open state follow the voltage dependence expected for a three-state gating scheme such as that of Eq. **1**. Furthermore, at saturation of the voltage-dependent rates, the individual channels are open only a small fraction of the time, as suggested by the single-channel data of Fig. 3.

To check that the noise does, indeed, emanate from several channels of the type seen in the single-channel patches, we calculate the ratio of variance-to-mean from the data of Fig. 6 as follows:

$$\mathrm{Var_I}(V)/\langle I\rangle(V - E) = \gamma(1 - p), \quad [7]$$

so that at each value of V, the ratio can be used to calculate γ. The result of this calculation for several values of V leads to an estimate of the unitary conductance, $\gamma = 17 \pm 5$ pS, consistent with the single-channel determination.

1. Serrano, R. (1985) In *Plasma Membrane ATPase of Plants and Fungi* (CRC Press, Boca Raton, FL), pp. 48–52.
2. Goffeau, A. & Slayman, C. W. (1981) *Biochim. Biophys. Acta* **639**, 197–223.
3. Serrano, R., Kielland-Brandt, M. C. & Fink, G. F. (1986) *Nature (London)* **319**, 689–693.
4. Rodriguez-Navarro, A. & Ramos, J. (1984) *J. Bacteriol.* **159**, 940–945.
5. Gustin, M. C., Martinac, B., Saimi, Y., Culbertson, M. & Kung, C. (1986) *Science* **233**, 1195–1197.
6. Hamill, O. P., Marty, A., Neher, E., Sakmann, B. & Sigworth, F. J. (1981) *Pflügers Arch.* **391**, 85–100.
7. McCusker, J. H., Perlin, D. S. & Haber, J. E. (1988) *Mol. Cell Biol.*, in press.
8. Perlin, D. S., Brown, C. & Haber, J. E. (1988) *J. Biol. Chem.*, in press.
9. Schroeder, J. I., Raschke, K. & Neher, E. (1987) *Proc. Natl. Acad. Sci. USA* **84**, 4108–4112.
10. Eddy, A. A. (1978) in *Current Topics in Membranes and Transport*, eds. Bronner, F. & Kleinzeller, A. (Academic, New York), Vol. 10, pp. 279–360.
11. Seaston, A., Carr, G. & Eddy, A. A. (1976) *Biochem. J.* **154**, 669–676.
12. Peña, A. (1975) *Arch. Biochem. Biophys.* **167**, 397–409.
13. Villalobo, A. (1982) *J. Biol. Chem.* **257**, 1824–1828.